IJCRT.ORG ISSN : 2320-2882

INTERNATIONAL JOURNAL OF CREATIVE RESEARCH THOUGHTS (IJCRT)

An International Open Access, Peer-reviewed, Refereed Journal

Performance Evaluation of a PV-Powered BLDC Motor Drive Using PSO-Based MPPT and Zeta DC–DC Converter for Electric Vehicle Applications

[1]Sandeep Kumar, [2]Ravinder Kaur, [3]Balwinder Singh

[1]M.Tech Student, [2]Asistant Professor, [32]Asistant Professor

[1]Department of Electrical Engineering,

[1]Guru Nanak Dev Engineering College Ludhiana, India

Abstract: This paper presents a performance evaluation of a photovoltaic (PV)-powered brushless direct-current (BLDC) motor drive for electric-vehicle propulsion. The developed system integrates a 1200 W PV array, particle swarm optimization (PSO)-based maximum power point tracking (MPPT), a Zeta DC–DC converter, a bidirectional buck–boost battery interface, a three-phase voltage-source inverter, and a BLDC motor. The PV source is modeled using a single-diode representation, while the PSO controller searches for the converter duty cycle that maximizes extracted PV power. The Zeta converter conditions the PV voltage and provides a regulated DC link, and the battery supports energy balance during changing requirements. MATLAB/Simulink simulation is used to examine PV characteristics, converter output, battery behavior, inverter operation, motor speed, torque, and speed transitions. At the operating condition, the PV array produces approximately 78 V, 15.2 A, and 1185 W, while the converter provides about 198 V, 5.1 A, and 1010 W. Battery voltage is maintained near 200 V, charging current is approximately 1.15 A, and SOC remains close to 62%. The BLDC drive demonstrates rapid speed tracking, with acceleration and deceleration settling times of 0.075 s and 0.082 s, respectively. These results demonstrate coordinated operation of the source, conversion stages, storage, and traction drive.

Index Terms **-** Photovoltaic system; BLDC motor; electric vehicle; PSO-MPPT; Zeta converter

1. Introduction

1.1 Background

Electric-vehicle propulsion is associated with efficient electrical drives and renewable energy integration. The proposed system describes solar photovoltaic generation as an energy source because it can supply power without direct dependence on conventional fuel-based generation. A PV-fed traction system, however, does not receive a fixed electrical input. PV voltage and current vary with irradiance and operating conditions, and the resulting nonlinear power characteristic contains a maximum-power operating point. Therefore, the usefulness of a PV source for a traction drive depends not only on the installed array but also on the ability of the power-conditioning system to extract and regulate available energy. The present work addresses this issue through a coordinated PV–converter–storage arrangement.

The BLDC motor is selected in the proposed system because of its high efficiency, compact construction, high power-to-weight capability, and low maintenance requirement. Electronic commutation using rotor-position feedback provides controllable motor operation and makes the machine suitable for dynamic drive requirements. For a PV-powered BLDC system, however, motor performance is closely linked to the quality of the DC supply. A reduction or fluctuation in PV power can influence the speed–torque response unless suitable power conditioning and storage are provided. The proposed system therefore combines a Zeta DC–DC converter with battery storage and a three-phase voltage-source inverter. The Zeta converter is used for voltage conditioning, while the battery provides support when the instantaneous solar contribution is insufficient.

1.2 Research Problem

The central research problem is the coordinated regulation of a nonlinear renewable source and a traction motor under changing electrical conditions. The PV array has a nonlinear voltage–current and power–voltage characteristic, so operation away from its maximum-power point causes available solar energy to be underutilized. At the same time, the BLDC motor requires a regulated DC-link supply to maintain the commanded speed. A direct connection between the two systems would therefore provide limited control over the operating point and could produce undesirable speed and torque variations during operation. The proposed system also identifies a need to coordinate the PV source, DC–DC converter, battery, inverter, and motor rather than treating them as independent subsystems.

The problem is further influenced by the dynamic behavior of the motor. Load changes and speed commands require the electrical drive to respond quickly while limiting steady-state error. Battery operation must also remain controlled so that excess solar energy can be stored and energy can be released when required. The study consequently considers MPPT, converter regulation, energy storage, and closed-loop motor control within one integrated simulation model. PSO is used to determine a suitable converter duty cycle for maximum PV power extraction, while the Zeta converter conditions the DC output and the motor controller regulates speed.

1.3 Research Objective

The objective of the work is to develop and evaluate an integrated PV-powered BLDC motor drive using PSO-based MPPT and a Zeta DC–DC converter for EV-oriented operation. The specific objectives are to: (i) model the PV source and characterize its voltage, current, and power behavior; (ii) implement PSO-based MPPT to identify the operating condition associated with maximum available PV power; (iii) evaluate the Zeta converter in terms of regulated output voltage, current, power, and ripple behavior; (iv) incorporate battery energy storage through a bidirectional buck–boost interface to support power balance; and (v) evaluate BLDC speed and torque behavior under variable load and speed-transition conditions. The proposed PV-powered BLDC drive system is modeled and simulated in MATLAB/Simulink using the system parameters summarized in Table I., including a 1200 W PV array, 78 V PV voltage, 1000 W/m² irradiance, 198 V converter output, 200 V battery, 20 Ah battery capacity, 3000 rpm rated motor speed, and PSO settings of 25 particles and 80 iterations. The outcome is an integrated assessment of the drive.

2. Literature Review

2.1 PV Modeling and MPPT Development

Previous research shows that PV modeling and MPPT remain fundamental to renewable motor-drive design. Salmi et al. presented a MATLAB/Simulink PV-cell model based on a single-diode equivalent circuit, demonstrating that PV behavior can be represented through a photocurrent source, diode, series resistance, and shunt resistance [1]. Rajani and Pandya compared Perturb and Observe and Incremental Conductance MPPT and reported better tracking during rapid irradiance changes for Incremental Conductance, while P&O showed operating-point oscillations [2]. De Brito et al. compared several MPPT methods using tracking efficiency, convergence speed, implementation complexity, and dynamic response as evaluation criteria [3]. Previous studies considered in the literature review include work on intelligent and optimization-based MPPT, including PSO-based control. Chamundeeswari and Seyezhai applied PSO to tune an MPPT controller using a LUO converter and reported faster convergence and improved converter performance [4]. These studies establish the value of adaptive or optimization-based tracking for nonlinear PV systems and provide the technical context for applying PSO to the present drive.

2.2 Converter and BLDC Drive Research

Previous research also emphasizes the importance of the power-conversion stage and motor-control loop. Sharma and Diwan modeled and controlled a Zeta converter in continuous conduction mode and reported step-up/step-down capability with reduced output ripple and improved voltage regulation [5]. Kumar and Singh investigated a solar-PV-fed BLDC motor drive using a boost converter, demonstrating the role of the intermediate converter in raising PV voltage to a usable level for the motor drive [6]. Kancherla and Kishore examined a solar-PV-operated DC–DC-converter-fed PMBLDC drive and reported stable motor operation and effective solar-energy utilization [7]. Lins and Krishnakumar investigated PSO- and TLBO-based tuning of a PID controller for a PV-fed BLDC motor and reported improved speed-tracking characteristics [8]. Collectively, these works indicate that PV modeling, MPPT, converter regulation, and BLDC control are interdependent design elements. The present study combines these elements with battery storage in one simulation framework and evaluates their coordinated behavior.The research-gap discussion in the source further notes that many studies examine PV modeling, MPPT, converters, or BLDC control separately, while coordinated system-level behavior under dynamic conditions is less extensively addressed. It also identifies limited comparative evaluation under identical operating conditions, incomplete treatment of battery coordination, and insufficient attention to maintaining a stable DC-link voltage during fluctuating PV input. These observations motivate an integrated simulation in which the MPPT output directly influences the converter, the converter interacts with the storage system, and the regulated link supplies the BLDC drive.

3. Methodology

3.1 PV Source and Zeta Converter Model

The simulation model is organized as a PV source followed by a PSO-controlled DC–DC conversion stage, battery storage, a three-phase voltage-source inverter, and a BLDC motor. The PV source uses the single-diode representation used in the developed system, in which photocurrent, diode behavior, series resistance, and shunt resistance determine the electrical response. The model is evaluated at 1000 W/m² irradiance with a rated PV power of 1200 W and a nominal PV voltage of 78 V. The PV operating point is characterized through voltage, current, and power responses so that the effect of MPPT can be observed directly.

The Zeta converter is selected as the principal PV power-conditioning stage. It contains the switching device, diode, inductors, and capacitors required for controlled energy transfer. During switching operation, the inductive elements store and release energy, while the converter duty cycle determines the regulated output. The developed model describes the converter as capable of both step-up and step-down voltage conversion with reduced output ripple. The simulated converter is configured for approximately 198 V output, providing the DC-link level required by the downstream inverter and motor drive.

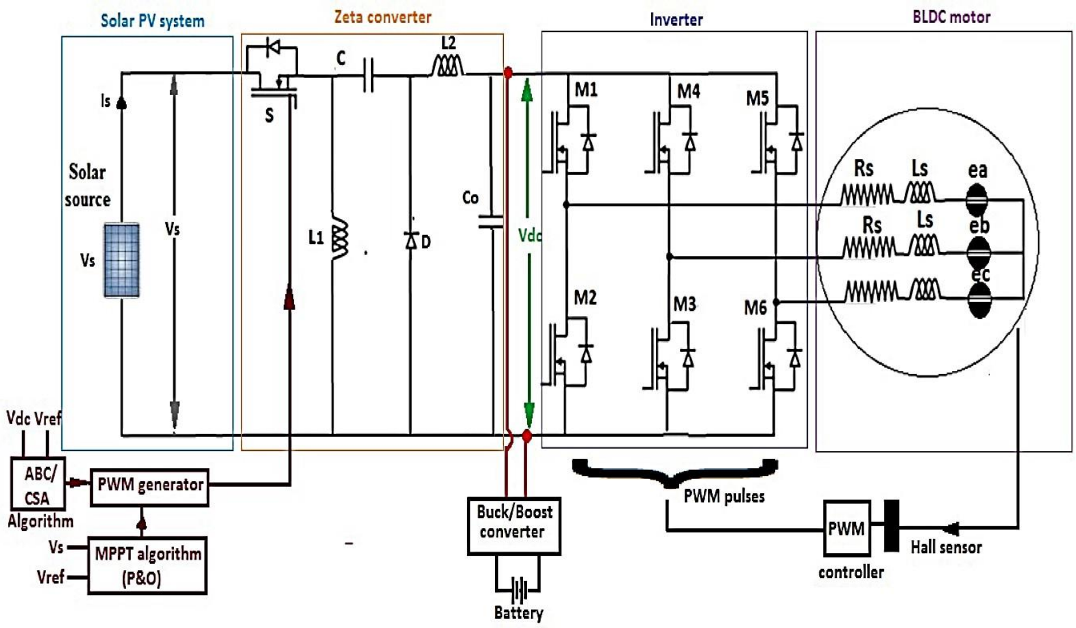

Fig. 1. Integrated topology of the PV-powered BLDC drive.

3.2 PSO-Based MPPT

PSO is applied as the MPPT mechanism by treating converter duty-cycle values as candidate particle positions. For each particle, the associated PV output power is evaluated as the fitness measure. Each particle retains its personal best position, while the swarm identifies a global best position. Particle velocity and position are then updated iteratively using the inertia weight, cognitive coefficient, social coefficient, and random terms. In the proposed configuration, the swarm contains 25 particles and the optimization is allowed to run for a maximum of 80 iterations. The inertia weight varies from 0.8 to 0.3, with cognitive and social coefficients of 1.8 and 2.1, respectively. The resulting best duty-cycle command is supplied to the converter switch, allowing the operating point to move toward the maximum available PV power.

The velocity update equation is expressed as

$$V_i(t+1) = W\,V_i(t) + C_1 r_1(Pbest_i - X_i(t)) + C_2 r_2(Gbest_i - X_i(t))$$

Position of the particle is modified as

$$X_i(t+1) = X_i(t) + V_i(t+1)$$

Where,

i = index of the particle

C_1, C_2 = acceleration constant

r_1, r_2 = random numbers ∈ (0,1)

t = no of iteration

W = Inertial Weight

V_i = velocity of the i^{th} particle

X_i = position of the i^{th} particle

Pbest = personal best of i^{th} particle

Gbest = Global best of i^{th} particle

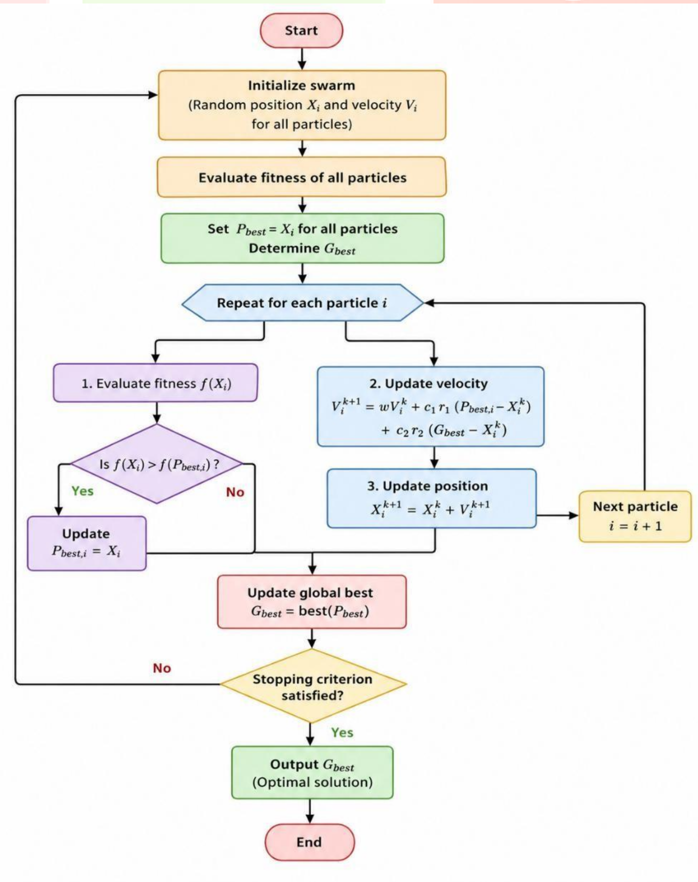

Fig No. 2. Block Diagram of Proposed PSO-BASED MPPT Control Scheme

3.3 Battery and BLDC Drive Control

The storage and traction subsystems complete the energy-management loop. A 200 V, 20 Ah battery is connected through a bidirectional buck–boost converter. In the charging direction, surplus PV energy is transferred to the battery; in the discharging direction, stored energy can support the load. Battery behavior is represented using terminal-voltage and SOC relationships for different charging and discharging current levels. The regulated DC output is applied to a three-phase VSI, which supplies the BLDC motor. Hall-sensor feedback determines rotor position for electronic commutation, while a closed-loop speed controller compares actual speed with the reference and adjusts the drive command. Performance is evaluated through PV voltage/current/power, converter voltage/current/power, battery voltage/current/SOC, inverter characteristics, motor speed, electromagnetic torque, and acceleration/deceleration response.

4. Present Work

4.1 System Configuration and Simulation Parameters

The implemented drive is treated as an integrated energy-conversion chain. The architecture contains the solar PV array, PSO-based MPPT controller, Zeta DC–DC converter, bidirectional battery interface, three-phase VSI, and BLDC motor. The PV array supplies the primary energy. The MPPT controller observes PV variables and modifies converter duty cycle so that the array operates close to its maximum-power region. The Zeta converter conditions the PV voltage for the DC link. A battery is connected through the bidirectional buck–boost stage so that energy can be stored when generation exceeds demand and supplied when PV power is insufficient. The VSI converts the regulated DC-link voltage into the three-phase supply required by the BLDC machine. Hall-sensor feedback supports electronic commutation, while the speed-control loop regulates the mechanical operating point.

The numerical configuration is defined by the selected system design parameters. The PV array rated power is 1200 W and the specified PV voltage is 78 V at 1000 W/m² irradiance. The converter output target is 198 V. The battery is rated at 200 V and 20 Ah. The inverter is a three-phase VSI and the BLDC motor rated speed is 3000 rpm. PSO uses 25 particles, 80 maximum iterations, an inertia weight range of 0.8–0.3, a cognitive coefficient of 1.8, and a social coefficient of 2.1.

The PSO search is embedded in the power-conditioning loop. Candidate duty cycles are evaluated from PV power, after which personal-best and global-best solutions guide particle updates. This makes the MPPT decision responsive to the simulated operating point rather than a fixed duty ratio. The developed model evaluates electrical and mechanical responses together, allowing power extraction effects to be followed through the converter, storage, inverter, and motor. The one-second waveforms show transient and steady behavior.

Table I. Simulation parameters used in the proposed model.

Parameter	Value
PV array rated power	1200 W
PV array voltage	78 V
Irradiance level	1000 W/m²
Converter output voltage	198 V
Battery voltage	200 V
Battery capacity	20 Ah
Inverter	Three-phase VSI
Rated motor speed	3000 rpm
PSO swarm size	25
Maximum iterations	80
Inertia weight	0.8 to 0.3
Cognitive coefficient	1.8
Social coefficient	2.1

4.2 PV Array and MPPT Response

Under the stated operating condition, the PV response shows a rapid transient followed by a nearly steady region. Fig. 2 shows PV voltage rising to approximately 78 V, while current settles near 15.2 A. The power response rises rapidly, exhibits a short transient peak, and then remains close to the available operating power. The reported result is approximately 1185 W, indicating that the PSO-based MPPT controller identifies and maintains a high-power operating region. The plotted waveforms show that the initial transient is concentrated in the early part of the one-second simulation window.

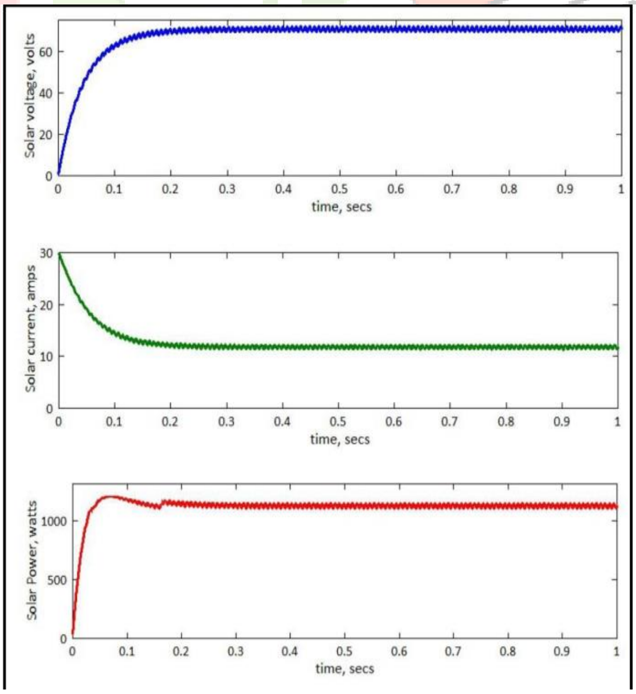

Fig. 2. PV voltage, current, and power response using PSO-based MPPT.

4.3 Zeta Converter Performance

Fig. 3 demonstrates the conditioning function of the Zeta stage. Output voltage rises toward approximately 198 V, while current approaches about 5.1 A. Output power is nearly 1010 W. The converter model operates continuous-conduction operation with reduced ripple. Thus, the converter provides a substantially higher DC voltage than the PV-side voltage while maintaining a regulated output suitable for the inverter. The difference between the reported PV input power and converter output power represents the modeled conversion loss and power-conditioning requirement; no additional efficiency value is inferred.

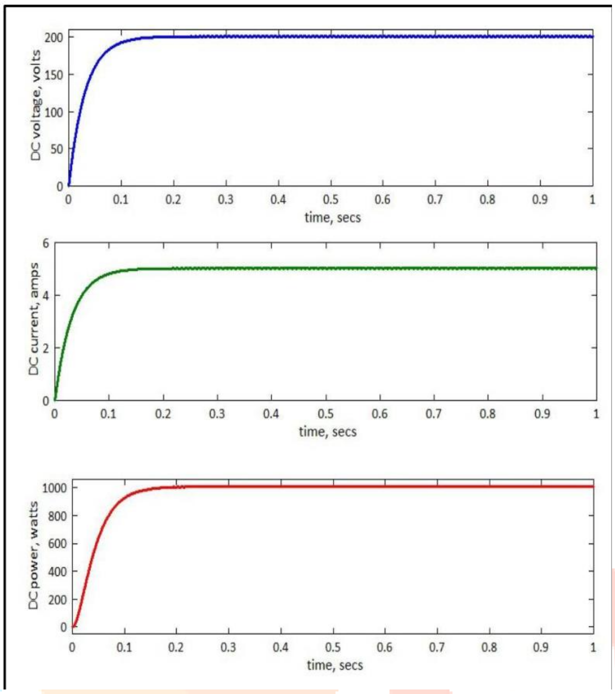

Fig. 3. Zeta converter output voltage, current, and power.

4.4 Battery Energy Storage and Operating Data

Fig. 4 presents battery voltage, charging current, and SOC. Battery voltage approaches and remains close to 200 V, while charging current settles around 1.15 A with switching-related variation. SOC rises and remains close to 62% during the later simulation interval. The battery operating data define terminal voltage against SOC for charging and discharging current levels. During discharge, the tabulated voltage increases from 199.3 V at 10% SOC and Cb/75 to 201.80 V at 100% SOC under that current condition; across the listed discharge currents, the 100% SOC voltage reaches 202.10 V at Cb/10. During charging, the 100% SOC voltage ranges from 201.80 V at Cb/50 to 202.10 V at Cb/10. These values provide the battery-model basis for controlled storage operation.

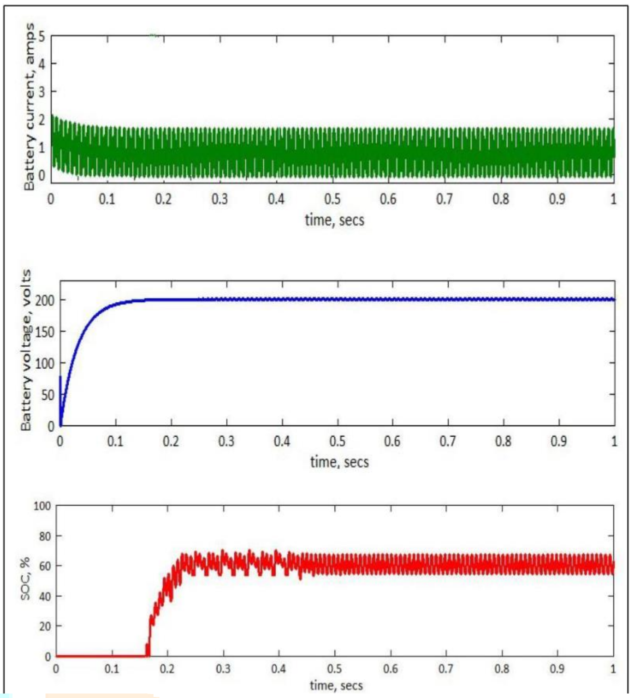

Fig. 4. Battery voltage, charging current, and state-of-charge response.

The battery model in the proposed system uses two separate terminal-voltage tables: one for discharging currents and one for charging currents. Both are retained separately below.

Table II(a). Terminal voltages at various discharging currents.

SOC	Voltage at Cb/75 (V)	Voltage at Cb/50 (V)	Voltage at Cb/30 (V)	Voltage at Cb/20 (V)	Voltage at Cb/10 (V)
10	199.30	199.25	199.28	199.65	200.05
20	200.30	200.32	200.35	200.40	200.45
30	200.45	200.52	200.55	200.60	200.65
40	200.65	200.68	200.70	200.75	200.85
50	200.85	200.90	200.92	200.95	201.00
60	201.00	201.05	201.08	201.12	201.18
70	201.25	201.30	201.35	201.40	201.45
80	201.45	201.52	201.58	201.60	201.65
90	201.65	201.70	201.75	201.78	201.85
100	201.80	201.85	201.90	201.95	202.10

Table II(b). Terminal voltages at various charging currents.

SOC	Voltage at Cb/50 (V)	Voltage at Cb/30 (V)	Voltage at Cb/20 (V)	Voltage at Cb/10 (V)
10	199.90	199.92	199.95	199.98
20	200.00	200.05	200.08	200.10
30	200.25	200.30	200.35	200.45
40	200.45	200.50	200.55	200.60
50	200.60	200.65	200.70	200.75
60	200.75	200.80	200.85	200.90
70	200.90	200.95	201.00	201.05
80	201.20	201.30	201.40	201.50
90	201.50	201.60	201.70	201.80
100	201.80	201.90	202.00	202.10

4.5 BLDC Drive and Dynamic Response

The traction stage converts the regulated DC supply for the BLDC motor. The modeled system provides balanced three-phase inverter operation with a peak voltage magnitude of approximately 200 V and phase currents close to 4 A. Stator currents have the expected quasi-square form, and the three-phase back-EMF waveforms are described as symmetrical. Fig. 5 shows rapid speed attainment followed by recovery from a variable-load disturbance. Fig. 6 shows a starting torque transient followed by a low-torque region and a higher torque response after the load event.

Quantitative data support these observations. Under no-load operation, the PSO controller gives a rise time of 0.05 s, settling time of 0.22 s, peak overshoot of 31%, and steady-state error of 0.06. Under full load, rise time is 0.03 s, settling time 0.21 s, overshoot 42%, and steady-state error 0.07. The higher full-load overshoot indicates a stronger transient response. Speed-transition tests provide an additional check. For acceleration from 2500 to 3000 rpm, rise time is 0.012 s, settling time 0.075 s, and overshoot 41%. For deceleration from 3000 to 2000 rpm, the values are 0.013 s, 0.082 s, and 40%. The close acceleration and deceleration times show rapid tracking of changing commands. Overall, the present work links PV extraction, converter regulation, battery support, inverter operation, and BLDC speed response within one MATLAB/Simulink framework.

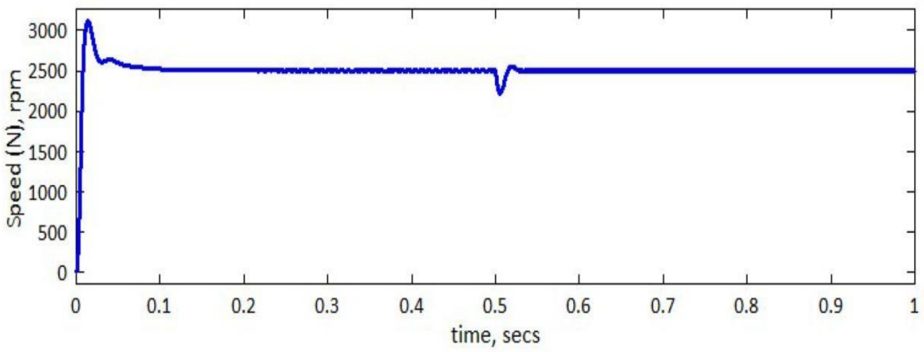

Fig. 5. BLDC motor speed response under variable load.

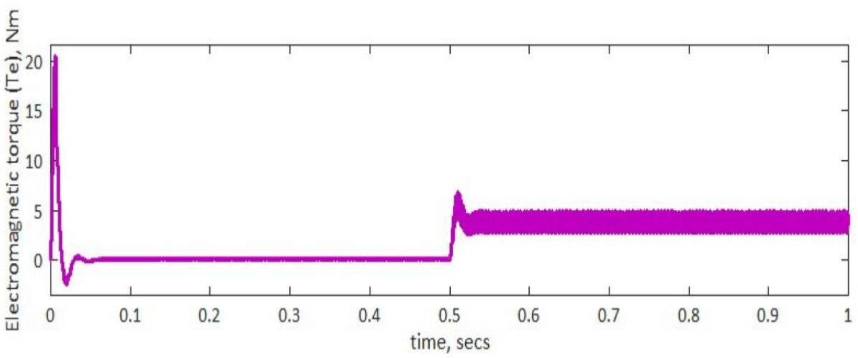

Fig. 6. Electromagnetic torque response of the BLDC motor.

Table III. BLDC dynamic performance under no-load and full-load conditions.

Operating condition	Rise time (s)	Settling time (s)	Peak overshoot (%)	Steady-state error
No load	0.05	0.22	31	0.06
Full load	0.03	0.21	42	0.07

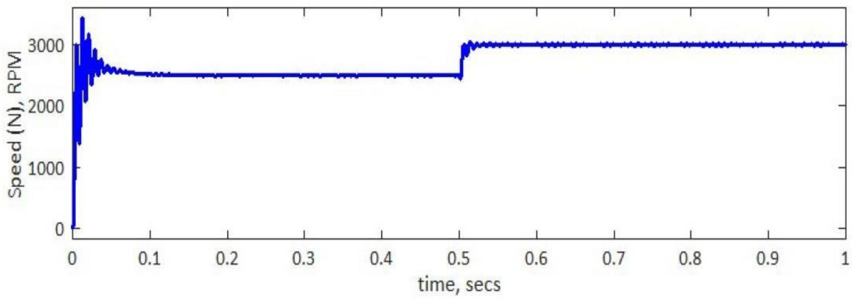

Fig. 7. BLDC speed response during acceleration transitions.

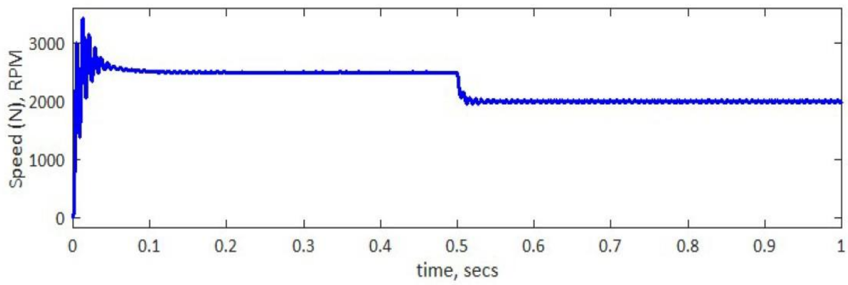

Fig. 8. BLDC speed response during deacceleration transitions.

Table IV. Dynamic characteristics during speed transition.

Operating mode	Reference-speed transition	Rise time (s)	Settling time (s)	Overshoot (%)
Acceleration	2500 → 3000 rpm	0.012	0.075	41
Deceleration	3000 → 2000 rpm	0.013	0.082	40

5. Results and Discussion

5.1 Results

The principal numerical results are summarized by the simulation waveforms and tables. The PV array reaches approximately 78 V, 15.2 A, and 1185 W. The Zeta converter raises the voltage to about 198 V and provides approximately 5.1 A and 1010 W. Battery voltage remains near 200 V, charging current is about 1.15 A, and SOC is close to 62%. The inverter operates with approximately 200 V peak voltage magnitude and phase currents near 4 A. The BLDC motor reaches the commanded speed region rapidly and recovers after the modeled load disturbance. The no-load and full-load dynamic indices are listed in Table III, while speed-transition indices are given in Table IV.

5.2 Discussion

The simulation results indicate that the proposed drive maintains coordinated electrical and mechanical operation under modeled operating condition. On the PV side, the PSO-based MPPT produces approximately 1185 W at about 78 V and 15.2 A. The waveform in Fig. 2 shows that the operating point reaches a stable region after initial transient, supporting the objective of extracting available solar power. The Zeta converter then raises the voltage to approximately 198 V and supplies about 5.1 A and 1010 W. This regulated DC output provides the electrical interface required by the inverter and demonstrates the role of converter in separating the PV operating point from the motor-side voltage requirement.

The storage results complement converter response. Battery voltage remains near 200 V, charging current is about 1.15 A, and SOC remains close to 62% during the simulation. This indicates that the battery model can absorb energy while maintaining the DC-side operating condition represented. On the traction side, the reported inverter voltage magnitude of about 200 V and phase currents near 4 A are consistent with the regulated link used to supply the BLDC motor. The speed response shows fast recovery after the load disturbance, while the torque waveform reflects the transient increase associated with load.

The numerical dynamic indices show a rise time of 0.05 s and settling time of 0.22 s at no load, compared with 0.03 s and 0.21 s at full load. Overshoot increases from 31% to 42%, while steady-state error changes from 0.06 to 0.07. During speed transitions, acceleration and deceleration settling times remain below 0.1 s. Overall, these results support the proposed system's conclusion that the coordinated PSO, converter, storage, and BLDC control structure provides satisfactory speed regulation and dynamic response. Since the reported results are simulation-based, the conclusions are limited to modeled conditions and parameters.

6. Future Scope

- Develop and test a hardware prototype using real PV panels, Zeta converter, battery storage, inverter, and BLDC motor to validate the simulated behavior under practical switching, thermal, and controller constraints.
- Compare PSO-based MPPT with fuzzy-logic, neural-network, genetic-algorithm, grey-wolf, and hybrid MPPT approaches using identical operating conditions.
- Evaluate the drive under broader temperature and irradiance variations, including rapid environmental changes, to examine MPPT robustness and energy-management performance.
- Extend the battery-management and bidirectional power-flow model toward regenerative braking, improved charge/discharge coordination, and real-time EV energy management.
- Implement the control strategy on a real-time platform such as an FPGA or DSP and investigate efficiency, cost, switching losses, thermal behavior, and practical controller response.

7. References

[1] T. Salmi, M. Bouzguenda, A. Gastli, and A. Masmoudi, "MATLAB/Simulink Based Modelling of Solar Photovoltaic Cell," International Journal of Renewable Energy Research, vol. 2, no. 2, pp. 213–218, 2012.

[2] S. V. Rajani and V. J. Pandya, "Comparison of P&O and Incremental Conductance MPPT Algorithms," Indian Academy of Sciences, 2015.

[3] M. A. G. De Brito et al., "Evaluation of MPPT Techniques for PV Applications," IEEE Transactions on Industrial Electronics, 2013.

[4] V. Chamundeeswari and R. Seyezhai, "PSO-PID MPPT Controller Using LUO Converter," PECCON, 2017.

[5] S. Sharma and R. Diwan, "Zeta Converter Modelling and Control," IJETT, 2019.

[6] R. Kumar and B. Singh, "BLDC Motor Driven Water Pump Fed by Solar PV Using Boost Converter," IEEE INDICON, 2015.

[7] A. B. Kancherla and D. R. Kishore, "Design of Solar-PV Operated DC–DC Converter Fed PMBLDC Motor Drive for Real-Time Applications," IEEE International Symposium on Sustainable Energy, Signal Processing and Cyber Security, pp. 1–6, 2020.

[8] A. W. Lins and R. Krishnakumar, "Tuning of PID Controller for a PV-Fed BLDC Motor Using PSO and TLBO Algorithm," Applied Nanoscience, vol. 13, no. 4, pp. 2911–2934, 2023.